Fuel 138 (2014) 1–14

Contents lists available at ScienceDirect

Fuel

journal homepage: www.elsevier.com/locate/fuel

Shrinkage kinetics of large-sized briquettes during pyrolysis and its application in tamped coal cakes from large-scale chambers

Qi Wang, Yuqiong Zhao, Yongfa Zhang *

Key Laboratory of Coal Science and Technology, Ministry of Education and Shanxi Province, Taiyuan University of Technology, Taiyuan, China

HIGHLIGHTS

- The shrink of large size briquette was studied by self-developed mass and volume integrated measuring device.
- The large size briquette shrinkage kinetic model during the pyrolysis process was established.
- The volume shrink calculation method of industrial tamped coal cake was obtained.

ARTICLE INFO

Article history:
Received 15 May 2014
Received in revised form 6 August 2014
Accepted 7 August 2014
Available online 24 August 2014

Keywords:
Briquette
Pyrolysis
Shrinkage
Kinetic models
Industrial application

ABSTRACT

Aiming at the general problem that both for the production of foundry coke made by anthracite pulverized coal and furnace coke made by tamped coke in the coke oven, namely the shrinkage problem for large-size briquette and tamped coke in the pyrolysis process, a mass and volume integrated measuring device was used to study the shrinkage process of large-sized briquettes (volume equals 10^3 cm^3) under constant temperature (450 °C, 550 °C, 650 °C and 850 °C). The briquette shrinkage kinetic model was also established according to the regulation of mass loss and volume shrinkage, where the volume shrink calculation method of tamped coal cakes (13,280 mm × 500 mm × 4300 mm) was also obtained. Three conclusions were drawn in this study: 1. In the process of the carbonization, the dehydration and degassing reaction before 450 °C as well as polycondensation reaction at 650 °C were the main reason causing the briquette shrinkage, the decomposition reaction at 550 °C came second, while the hydrogen evolution reaction after 850 °C has the least effect on briquette volume shrinkage. There were three main reasons causing the shrinkage of large-size briquette: the decrease of coal volume caused by the volatilization of moisture and volatiles, the decrease of coal volume caused by the pyrolysis reaction and the density increase of briquette caused by the decrease of coal volume. 2. The briquette shrinkage kinetic model was represented as follows: $dV_t/dt = V_0[(1-x)d\beta/dt - A_0e^{-E/RT}(1-x)^n\beta]$; There was a positive correlation between the volume changing parameter β and the density of briquette, and the volume changing parameter increased with the reaction; the shrinkage reaction was divided into three stages; with the reaction went on, the reaction order and reaction rate constant decreased, the pre-exponential factor increased and the activation energy decreased firstly and increased then. 3. The shrinkage of the tamped coal cakes from the large-scale chamber was counted in the calculated unit whose thickness was 100 mm. The shrinkage velocity of the tamped coal cakes in carbonization chamber was obtained by weighted calculating the shrinkage parameters of each volume unit at different temperatures. The shrink regulations of the tamped coal cakes in the carbonization chambers, which were in agreement with industrial production, were approximately the same as those of the large-sized briquettes. However, the shrinkage rate curve of the tamped coal cake in the carbonization chamber was gentler than that of the large-sized briquette, as a result of the large temperature gradient of different coal in carbonization chamber.

© 2014 Elsevier Ltd. All rights reserved.

1. Introduction

There are about 100 million tons of high rank pulverized coal burned to make electricity every year, making resource utilization unreasonable [1]. The material of foundry coke, high-quality coking coal and fat coal, is turning down. As a result, using the high rank pulverized coal as the material to make carbonization briquette will expand the type of coking coal and relieve the environmental pollution at the same time [2]. Co-coking is commonly used in the production of tamped coke in the large-scale coke oven,

* Corresponding author.

http://dx.doi.org/10.1016/j.fuel.2014.08.021
0016-2361/© 2014 Elsevier Ltd. All rights reserved.

Nomenclature

V	the volume of briquette (m^3)
W	the weight of briquette (g)
V'	the volume of coal in carbonization chamber (m^3)
t	carbonation time (s)
T	carbonation temperature (K)
β	the volume changing parameter
x	the conversion rate (%)
k	the reaction rate constant
A_0	the pre-exponential factor
E	the activation energy (J/mol)
R	ideal gas law constant, =8.314 J/mol K
n	the reaction order

Subscripts

a	The width parts of tamped coke in the carbonization chamber that been divided
i	the volume unit number of coal material in the carbonization chamber
0	the physical quantities at the initial time point
t	the physical quantities at the time t
f	the physical quantities at the end of the reaction

Defined parameter

V_t/V_0	the proportion of V_t in V_0
$\Delta V_t/V_0$	the result of V_t/V_0 at high temperature minus the V_t/V_0 at its lower neighbor temperature
p	the proportion of the shrinkage degree ($\Delta V_t/V_0$) at different temperature zones accounting for the total briquette shrinkage at 850 °C

thus the shrinkage characteristic will be the basis to guide the production of large-scale coke oven further. Using anthracite or meagre pulverized coal as the material to make carbonization briquette and tamped coke cleanly is an important technological approaches to use high rank pulverized coal and save precious coking coal resource scientifically and efficiently.

The shrinkage characteristics of high-temperature heat-treated briquettes have a direct effect on processes such as the discharge of the carbonized briquette, which has been widely studied [3–5]. The properties of coal and carbonization conditions influence briquette shrinkage. The properties of coal include the coal type (e.g., volatile and maceral), binder properties, the content of inert material and the molding density. The volume shrinkage rate increases linearly with the increase of coal blending volatiles [6–8]. Of the three primary types of macerals, inertinite promotes briquette shrinkage, vitrinite has no obvious relation to the briquette shrinkage, while heating vitrinite promotes briquette expansion [9,10]; binder types have a significant effect on the volume change rate of the briquettes, and the high ash content binder increases the shrinkage level of the first shrinkage peak after it is heated and solidified [9]. Adding inert materials, such as coke breeze also reduce the briquette shrinkage rate/contraction coefficient [11–13]. In addition, the briquette shrinkage rate increases with the compaction density [14–16]. The carbonization conditions include the heating rate, furnace temperature and carbonization time, among others. The radial shrinkage rate increases with the heating rate, which has little effect on briquette shrinkage in the low temperature zone (approximately 500–750 °C), while the effect in the high temperature zone (approximately 750–960 °C) is significant [17]. The furnace temperature and carbonization temperature influence the briquette shrinkage primarily by heating, which has an effect on fissure formation and coke density [11].

There are two shrinkage rate peaks during the coal carbonization process. First, the coal undergoes a drastic decomposition reaction, precipitating mostly tar and heavy hydrocarbon gas; the second decomposition process occurs in the solid phase and primarily, precipitates hydrogen [18]. Recent studies suggest that the free radical concentration of anthracite increases in the heating process, and the free radicals combine or undergo the polycondensation reaction with the binder [19]. The shrinkage is caused by the free radical fragment orientation and the crystalline ordered array [17]. The coal shrinkage process can be divided into three stages: slow contraction stage, transitional contraction stage, and rapid contraction stage, whose activation energy, pre exponential factor and rate constant increase in stages.

The shrinkage of coal during the process of heat treatment affects its pore structure [18], reactivity [19], crack formation [20,21], strength [22] and size distribution [23], which has a direct relationship with gasification characteristics of carbonized briquettes. Recently, the research of powdered coal used to make carbonized briquettes for the gasification industry has increased. Currently, researchers have focused on single coal particles or small-sized briquettes (volume smaller than 10^3 mm^3), and there are no published studies on the shrinkage characteristics, mechanism and kinetics of large-sized briquettes. However, studying the shrinkage characteristics of large-sized briquettes is imperative for the industrial use of briquettes. Thus, a mass and volume integrated measuring device was used to study the shrinkage process of large-sized briquette (volume equals 10^3 cm^3) under constant temperature(450 °C, 550 °C, 650 °C and 850 °C). The briquette shrinkage kinetic model was also established according to the regulation of mass loss and volume shrinkage, where the volume shrinkage calculation method of tamped coal cakes (13,280 mm × 500 mm × 4300 mm) was also obtained.

2. Experimental

2.1. Raw materials

Jincheng anthracite (JA) and Modified coal-based binder (MB) was used in this experiment. The proximate and ultimate analysis dates are shown in Table 1.

2.2. Mass loss measurement of large-sized briquette shrinkage

The anthracite coal and binder were crushed by 60 and 200 orders of magnitude, respectively. The anthracite and binder were mixed according to a certain proportion, and quantitative amounts of water were poured into the mixture and stirred. The mixture was put into a cube steel mold (100 mm × 100 mm × 100 mm) and the large compound briquettes were obtained.

The mass and volume integrated measuring device was used in this experiment during the pyrolysis process at high temperatures and atmospheric pressure (Fig. 1). The measuring device contained as quality measurement, volume measurement and signal processing unit, which could concurrently obtain the measurements of the large-sized briquette's mass loss and volume shrinkage; the sensitivity of mass loss and volume change measurements are 0.1 g and 0.1 mm respectively [24].

Table 1
Proximate analysis and ultimate analysis of raw material.

Sample	Proximate analysis (wt.%)				Ultimate analysis (wt.%)			
	M_{ad}	A_{ad}	V_{ad}	C_{daf}	H_{daf}	O_{daf}	N_{daf}	S_{daf}
Jincheng anthracite (JA)	9.99	11.44	7.51	92.74	2.89	2.49	0.87	1.01
Modified coal-based binder (MB)	0.96	13.46	27.49	83.49	3.18	12.38	0.88	0.07

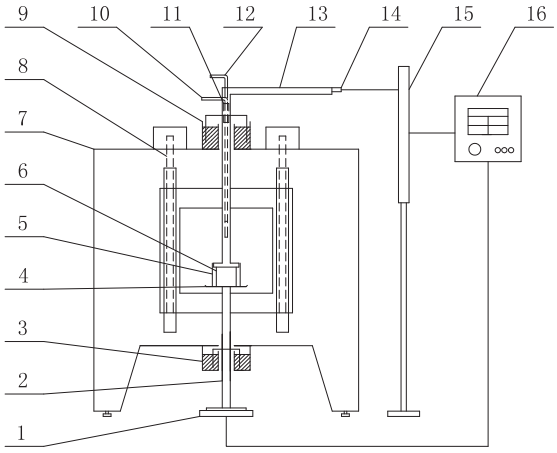

Fig. 1. The mass and volume integrated measuring device during the pyrolysis process at high temperature and ordinary pressure atmosphere, 1: mass sensor; 2: mass measuring rod; 3: the down liquid seal unit; 4: tray; 5: retort; 6: briquette; 7: furnace body; 8: Silicon carbide; 9: the upper liquid seal unit; 10: air-inlet duct; 11: temperature sensor; 12: exhaust duct; 13: volume measuring rod; 14: the light source; 15: light sensor; 16: display and control panel.

Different large-sized briquettes were heated to 450 °C, 550 °C, 650 °C and 850 °C and their mass loss and volume change was recorded. The temperature was kept constant and the experiment was stopped when the volume change and mass loss were less than 1 mm and 0.1 g, respectively. The regulation of the volume change and mass loss of the briquettes was measured at different heating rates.

2.3. Shrinkage measurement of coal in carbonization chamber

The industrial experiment for the shrinkage model was performed in a TJL4350D stamping coke oven, whose size parameters is shown in Table 2. Put the coal in the coal blending ratio that as the briquette's into the chambers. The coal and coke positions were measured in the tamping coke oven and the coal volume shrinkage rate was obtained.

2.4. The evaluation of parameters

2.4.1. Sensitivity analysis [25]

Sensitivity analysis is commonly employed to assess that in the nonlinear parameter estimation, and the nonlinear parameter estimation is usually carried out by using the least squares method in order to find the global minimum of the following objective function:

$$\mathrm{SSE} = \sum_{i=1}^{N\_data} \left(\frac{\mathrm{d}V}{\mathrm{d}t}_{exp} - \frac{\mathrm{d}V}{\mathrm{d}t}_{calc} \right)^2 \quad (1)$$

Sensitivity analysis is applied to each of the estimated parameters by means of perturbations of the parameter value (keeping the other parameters in their estimated values). Perturbations are preferably done in the range of ±20%. For each perturbation in the parameter values the objective function (the volume shrinkage rate equation) is reevaluated and then for each parameter the perturbation percentage is plotted against the corresponding value of the objective function. If all perturbations in all the parameters give the minimum of the objective function with their original values (0% perturbation), then the global minimum has been achieved. On the contrary, if at least one parameter does not give the same minimum than the others at 0% perturbation, that means poor nonlinear parameter estimation. To correct this, the values of the wrong estimated parameters are re-determined by examining the sensitivity plot, and finally, parameter sensitivity is carried out again on these parameters and now the global minimum is guaranteed.

2.4.2. Residual analysis

Calculate the briquette shrinkage rate difference between the experimental value and optimized value to investigation the proximity of them.

$$\mathrm{Residual} = \frac{\mathrm{d}V}{\mathrm{d}t}_{exp} - \frac{\mathrm{d}V}{\mathrm{d}t}_{opt} \quad (2)$$

2.4.3. Parity plots analysis

A parity plot is a scatterplot that compares expected data against experimental data. Each point has coordinates (x, y), where x is the experimental value of the volume shrinkage rate, and y is the corresponding optimized value. A line of the equation $y = x$ is added as a reference.

Table 2
Size parameters of carbonization chamber.

Working length (mm)	Width (pusher side, mm)	Width (coke side, mm)	Width average (mm)	Height (mm)
13,280	495	505	500	4300

3. Results and discussion

3.1. Briquette shrinkage kinetic analysis during the carbonization process

3.1.1. Shrinkage process analysis of large-sized briquettes

The briquette shrinkage curves at different carbonization temperatures are shown in Fig. 2a. The proportion of V_t in V_0 is represented by V_t/V_0. The V_t/V_0 at high temperature minus the V_t/V_0 at its higher neighbor temperature, then the $\Delta V_t/V_0$ is obtained. The proportion of the shrinkage degree ($\Delta V_t/V_0$) at different temperature zones accounting for the total briquette shrinkage at 850 °C was p.

As can be seen from Table 3, the value of p at 450 °C is large, dehydration and degassing reaction is the main reaction before 450 °C [24,26]. The free water of briquette is evaporated by heat, which will not cause the volume shrinkage of briquette directly. Only a certain volatilization extent of free water will lead to measurable volume shrinkage [27]. The decrease of coal volume caused

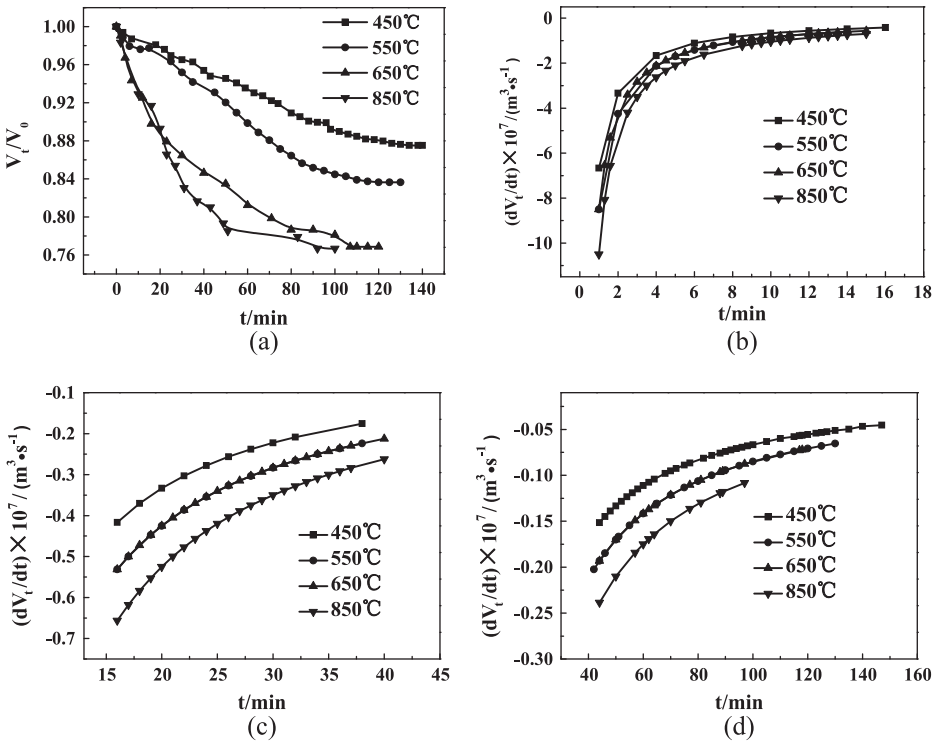

Fig. 2. Changing curves of briquette volume with time (a) shrinkage curves; (b) shrinkage rate curve (0–15 min); (c) shrinkage rate curve (15–40 min); (d) shrinkage rate curve (40–140 min).

Table 3
Parameters at different carbonation temperatures.

T (°C)	(V_t/V_0) (%)	$(\Delta V_t/V_0)$ (%)	p (%)
450	87.96	12.04	51.63
550	83.64	4.32	18.52
650	76.86	6.78	29.07
850	76.68	0.18	0.77

by the volatilization of moisture and volatiles and the decrease of coal volume caused by the pyrolysis reaction are the main reason causing the shrinkage of large-size briquette. Decomposition and condensation reactions carried out in the range of 450–550 °C and 550–650 °C separately. The decrease of coal volume caused by the pyrolysis reaction and the density increase of briquette caused by the decrease of coal volume are the main reasons causing the shrinkage of large-size briquette. The p at 850 °C was 0.77%; the gas precipitation decreased during this period, which was the least important factor causing the shrinkage.

Fig. 2b–d shows the briquette shrinkage rate curves under different carbonization temperatures. The instantaneous shrinkage rates of the large-sized briquettes were infinite, and the initial shrinkage rate was calculated according to the reaction values. When the reaction was stable, the shrinkage rate decreased rapidly in a short time period. A period later, the briquettes were in the slow shrinkage stage, and the shrinkage rates gradually decreased.

3.1.2. Establishing the shrinkage model

Under constant temperature, the volume of the briquette made under same conditions at time $t(V_t)$ was only related to the initial volume V_0 and the conversion x. Under the same initial volume, the larger the conversion, the smaller the V_t. Therefore, the briquette volume at time $t(V_t)$ had a positive correlation with the residual rate $1-x$, i.e., $V_t \propto V_0(1-x)$, and the parameter β was introduced to describe the volume during briquette pyrolysis process:

$$V_t = V_0(1-x)\beta \tag{3}$$

where β is the volume changing parameter during the briquette pyrolysis process, which varies with time and temperature.

Under constant temperature, the relationship of the volume change rate, conversion and volume change coefficient is obtained by derivation of Eq. (3):

$$dV_t/dt = V_0[-(dx/dt)\beta + (1-x)d\beta/dt] \tag{4}$$

where combined with the Arrhenius equation

$$k = A_0 e^{-E/RT} \tag{5}$$

and the shrinking core model

$$\frac{dx}{dt} = k(1-x)^n \tag{6}$$

the shrinkage kinetic model is obtained

$$dV_t/dt = V_0[(1-x)d\beta/dt - A_0 e^{-E/RT}(1-x)^n\beta] \tag{7}$$

The term volume changing parameter is obtained by Eq. (3), and described as follows:

$$\beta = V_t/[V_0(1-x)] \tag{8}$$

3.1.3. Verification of the shrinkage model

The variation in the regulation of the briquette volume and mass under constant temperature was obtained by experiment. The theoretical value of dV_t/dt was obtained through Eq. (7), and by derivation of the equation between the briquette volume and time, the experiment value of dV_t/dt was obtained. The theoretical and experiment value are explained in Sections 3.1.3.1 (calculation of theoretical value) and 3.1.3.2 (calculation of experimental value) below respectively.

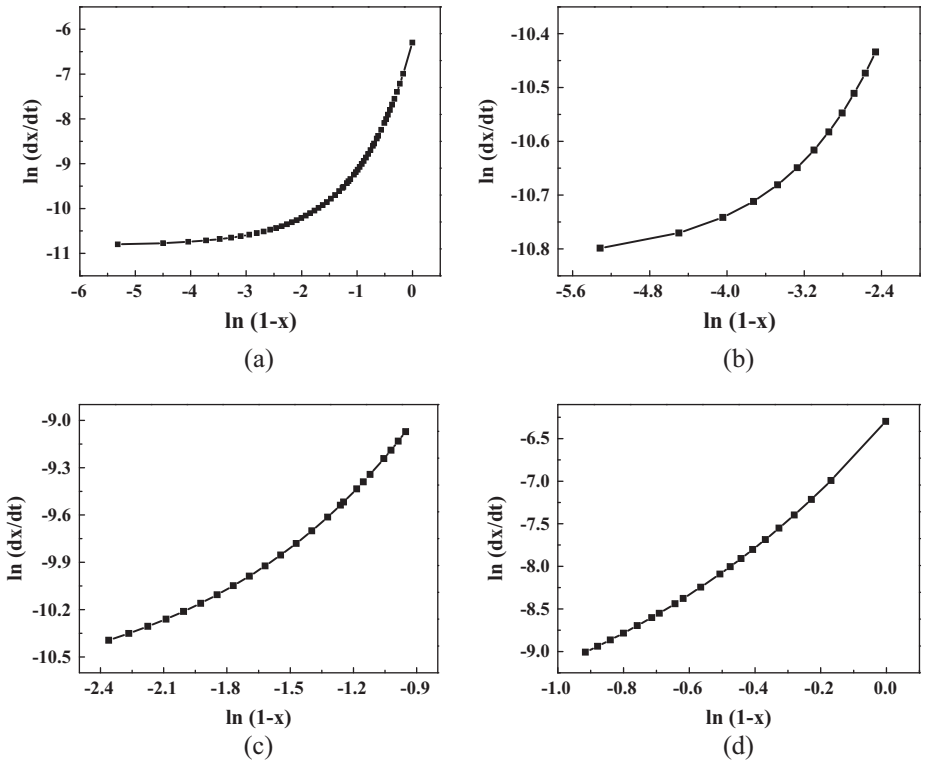

Fig. 3. Relation graphs of $\ln(1-x)$ and $\ln(dx/dt)$ under 550 °C: (a) the diagram of whole time and (b–d) the diagram of each time.

3.1.3.1. The calculation of theoretical value. The linear equations are obtained by taking the logarithm on both sides of the shrinking core model (Eq. (4)).

$$\ln(dx/dt) = n\ln(1-x) + \ln k \tag{9}$$

where x is the briquette conversion, $x = (W_0 - W_t)/(W_0 - W_f)$ (%), W_0 is briquette mass at the initial time point (g), W_t is briquette mass at the time t (g), W_f is briquette mass at the end of the reaction (g), k is obtained by the Arrhenius equation ($k = A_0 e^{-E/RT}$), where A_0 is the pre-exponential factor (s^{-1}), E is the activation energy (J/mol); R is the ideal gas law constant (J/(mol K)), T is reaction temperature (K), t is reaction time (s), and n is reaction order.

Eq. (9) was used to draw curves of $\ln(1-x)$ on $\ln(dx/dt)$, using the line slope and intercept to obtain the reaction order n and coefficient k [24]. The $\ln(1-x)$ to $\ln(dx/dt)$ curve at 550 °C during the briquette pyrolysis is shown in Fig. 3a; their relationship was nonlinear, and the curve was divided into three straight lines according to the approximate reaction stage. The graphs can be seen in Fig. 3b–d.

The related graphs of $\ln(1-x)$ and $\ln(dx/dt)$ at other temperatures were similar to the graphs at 550 °C. The reaction order n and the coefficient k at different temperature stages are shown in Table 4. The reaction order decreased gradually with the reaction at the same temperature.

The reaction order decreased with the reaction time at the same temperature, and that is similar to the change regulation of briquette pyrolysis parameters. Pitt [28] figured out that the devolatilization of coal is a series of parallel first order reaction. A heating process is needed for briquette to reach the reaction temperature in the first period, and there are kinds of parallel reactions, thus the apparent reaction order is large. With the time goes by, the apparent reaction order decreases with the decrease of reaction kinds.

The reaction rate constant decreases with the reaction. The reaction rate constant reflects the shrinkage speed of briquette to

Table 4
Shrinkage kinetic parameters of briquette at different reaction temperature.

Time (h)	T_1 (°C)	n_1	$k_1 \times 10^5$	R^2	T_2 (°C)	n_2	$k_2 \times 10^5$	R^2
0–2		2.580	77.962	0.947		2.627	83.950	0.950
2–5	450	0.625	5.837	0.952	460	0.788	8.317	0.987
5–5.8		0.165	1.675	0.985		0.153	1.699	0.980
0–1.25		2.819	139.634	0.982		2.877	142.500	0.983
1.25–3	550	0.946	24.750	0.969	560	0.948	24.777	0.969
3–4.5		0.129	3.766	0.867		0.132	3.796	0.872
0–0.5		2.838	86.205	0.981		2.835	86.403	0.983
0.5–2	650	1.306	16.571	0.992	660	1.306	16.576	0.992
2–3		0.694	5.617	0.995		0.706	5.760	0.994
0–0.5		2.970	419.736	0.936		2.997	424.124	0.938
0.5–0.85	850	1.010	42.391	0.995	860	1.015	42.514	0.995
0.85–1.4		0.457	14.373	0.988		0.462	14.468	0.988

Table 5
Kinetic parameters of briquette shrinkage at different reaction temperatures.

T (°C)	Time (h)	$A_0 \times 10^{-3}$	E (J mol^{-1})	β
450	0–2	0.910	56,077	$\frac{1.248-0.040\ln t}{1.961-0.195\ln t}$
	2–5	5.694	2618	
	5–5.8	21.388	6271	
550	0–1.25	0.132	11,585	$\frac{1.301-0.051\ln t}{2.054-0.221\ln t}$
	1.25–3	3.687	622	
	3–4.5	13.636	4524	
650	0–0.5	0.936	10,643	$\frac{1.299-0.059\ln t}{1.819-0.178\ln t}$
	0.5–2	5.868	216	
	2–3	7.695	5005	
850	0–0.5	0.081	9140	$\frac{1.313-0.063\ln t}{1.707-0.194\ln t}$
	0.5–0.85	1.748	2546	
	0.85–1.4	3.518	5800	

Table 6
The expression of briquette volume and briquette volume shrinkage rate at different reaction temperatures.

T (°C)	V_t/V_0	$(dV/dt) \times 10^3$ (m^3 s^{-1})	
		Experimental value	Theoretical value
450	$-0.040\ln t + 1.248$	$-\frac{0.040}{t}$	$-\frac{1}{23.83t+3059}$
550	$-0.051\ln t + 1.301$	$-\frac{0.051}{t}$	$-\frac{1}{19.82t+2288}$
650	$-0.059\ln t + 1.299$	$-\frac{0.059}{t}$	$-\frac{1}{15.60t+1840}$
850	$-0.063\ln t + 1.313$	$-\frac{0.063}{t}$	$-\frac{1}{12.13t+1271}$

some extent. At the initial stage of the reaction, the volatilization of moisture and volatile leads to rapid volume shrinkage; the reaction rate constant decreased gradually along with the reaction then. The results can be also explained by the content in Section 3.1.1. The activation energy and the pre-exponential factor at two similar temperatures were approximately the same, which was obtained by the Arrhenius equation through the calculation of the k value. Two similar temperatures represented by T_1 and T_2 ($T_2 = T_1 + 10$) showed a coefficient k at temperature T_1 and T_2; the first stages are k_1 a and k_2 as seen below:

$$k_1 = A_0 e^{-E/RT_1} \tag{10}$$

$$k_2 = A_0 e^{-E/RT_2} \tag{11}$$

The activation energy of the first stage at temperature T_1 is represented by the following:

$$E = RT_1T_2/(T_1 - T_2)\ln(k_1/k_2) \tag{12}$$

Bring the calculated activation energy E into Eq. (10); the corresponding pre exponential factor A_0 is obtained. Bring the conversion of briquette into Eq. (8), the volume changing parameter β under different temperatures are obtained. The activation energy E, pre exponential factor A_0 and the volume change parameter β of different stages and temperatures are shown in Table 5.

Under the same temperature, the pre-exponential factor increased with the reaction. And that is similar to the change regulation of briquette pyrolysis parameters. From the collision theory, the pre-exponential factor represents the collision frequency of the molecules. The molecular collision frequency increases with increasing temperature.

The activation energy of large-size briquette decreased firstly and increased then. That is different from the change regulation of briquette pyrolysis parameters [29,30]. Only a certain volatilization extent of free water will lead to measurable volume shrinkage, thus the apparent activation energy of first stage is large. The shrinkage of briquette is mainly caused by the pyrolysis of coal in the second and third stages; as a result, the pyrolysis activation energy represents the shrinkage activation energy in some extent. The pyrolysis activation energy increases with the reaction, and so as the shrinkage activation energy.

The volume changing parameters of large-size briquette increases with the time. And there was a positive correlation between the volume changing parameter β and the density of briquette as can be seen from Eq. (13).

$$\beta = \frac{V_t}{V_0(1-x)} \propto \frac{V_0}{W_0} \times \frac{V_t}{V_0(1-x)} = \frac{V_t}{W_0(1-x)} \propto \frac{V_t}{W_t} = \rho_t \tag{13}$$

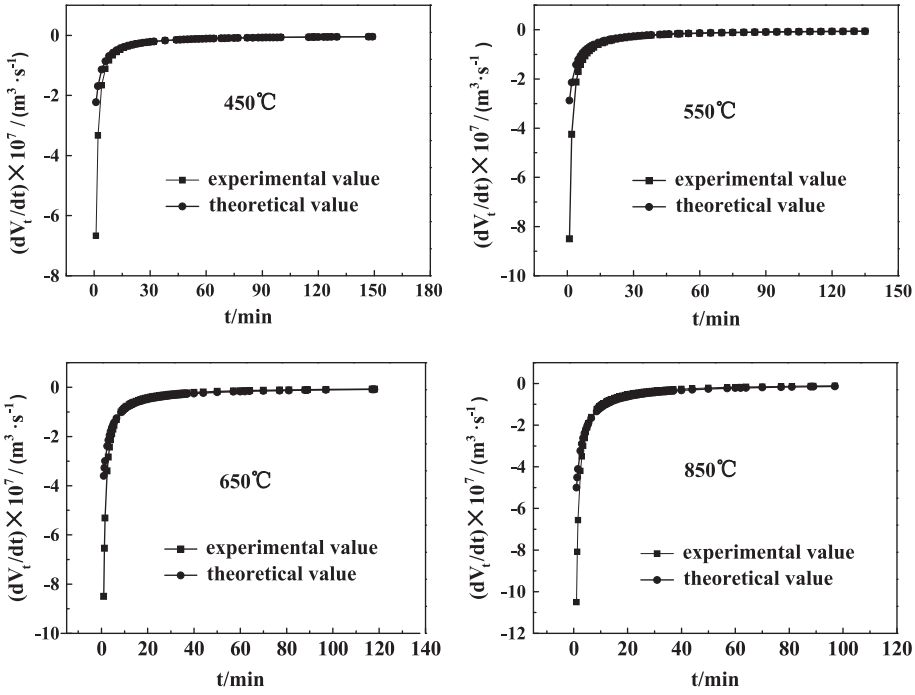

Fig. 4. Comparison of experimental and theoretical values at different temperatures.

The pyrolysis kinetic parameters of briquette was calculated on the basis of mass loss change regulation, while the shrinkage kinetic parameters of briquette was calculated on the basis of the volume change regulation; different kinetic model basis was the main reason that cause the difference between the kinetic parameter change regulation of the two kinetic model.

Bring the shrinkage kinetic parameters of briquette into Eq. (7) to calculate theoretical value of briquette shrinkage rate, and the relational expression of theoretical value was obtained (Table 6)

3.1.3.2. The calculation of experimental value. According to the briquette shrinkage curve at different temperatures in Fig. 2a, the briquette volume shrinkage regulation was obtained. The experimental value of dV/dt is acquired through the differential of briquette volume shrinkage regulation. The results are shown in Table 6.

The experimental and theoretical values of dV_t/dt at different temperatures are shown in Fig. 4, and the results are consistent.

3.1.3.3. The evaluation of kinetic parameters. As the volume changing parameter β was obtained through the calculation of experimental value directly, the sensitive analysis was only practiced for pre exponential factor A_0, activation energy E and the reaction order n at 450 °C, 550 °C, 650 °C and 850 °C. The residual analysis and parity plots analysis was employed to compare the difference among experimental value and optimized value [25].

As the kinetic model is divided into three sections, the sensitivity analysis will be carried out in three sections too. For each perturbation in each parameter, the objective function was evaluated and the results are presented in Fig. 5. The mark of 450 °C-1 represents the first stage of reaction at 450 °C, and the other marks have the similar meaning.

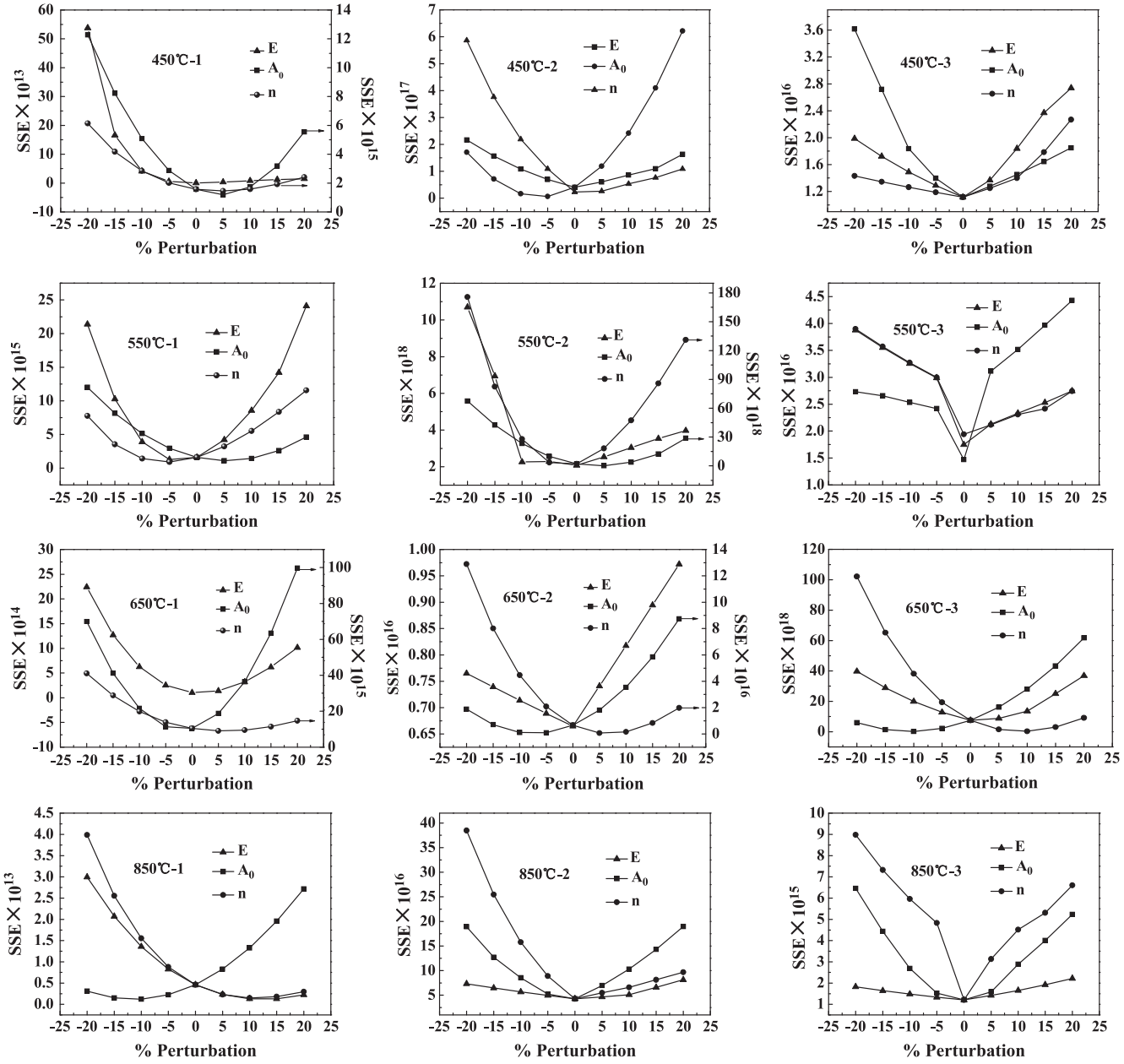

Fig. 5. Sensitivity analysis of kinetic parameters at different temperatures and during different time period.

From Fig. 5 it is clearly seen that the some estimated parameters (such as the curves in figure 450 °C-3) are the optimum since at 0% perturbation the SSE is the minimum, which is the condition to assure the correct values of parameters. Some parameters in these figures (such as the A_0 curve in figure 450 °C-2) do not show the least SSE at 0% perturbation, and then optimized procedures are needed. Fig. 6 finds the optimized value by graphic visualization.

The optimized value of kinetic parameters is shown in Table 7.

With the optimized values of kinetic parameters sensitivity analysis is performed again and the results are shown in Fig. 7.

The residuals analysis and parity plot analysis of four temperatures are shown in Figs. 8 and 9 respectively. The shrinkage kinetic model of large-size briquette in the pyrolysis process is in good agreement with the experimental value.

3.2. Industrial amplification of the shrinkage model

3.2.1. Establishing the carbonization chamber shrinkage model

The coal material from the carbonization chamber was divided into a parts, and labeled 1, 2, 3, ... i ..., a from left to right. The initial volume of coal labeled a was V'_{0i} (m^3), and the volume of coal at time t was V'_{ti} (m^3). In industrial production, the coal in the carbonization chamber is heated by the combustion chamber on its two sides, which was similar to the way the large-sized briquettes were heated in this study. The average width of the carbonization chamber was 500 mm. To obtain the volume units, the carbonization chamber was divided into 10 parts by the width, namely the parameters were adjusted from a to 10; thus, the coal labeled i and $a - i + 1$ represented the volume unit, and the volume shrinkage could be evaluated by the shrinkage of the briquettes

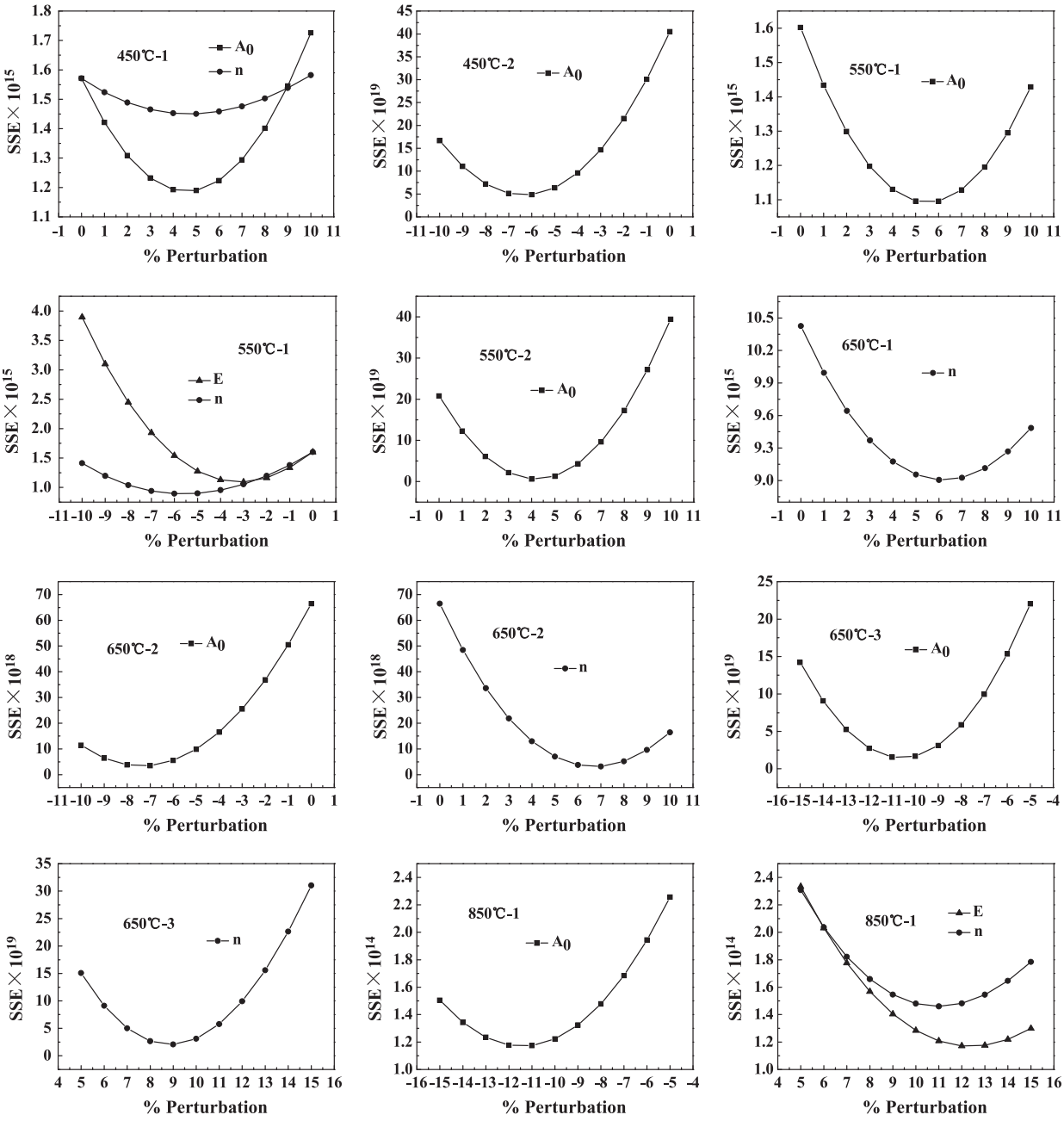

Fig. 6. Secondary sensitivity analysis of kinetic parameters at different temperatures and during different time period.

Table 7
The theoretical value and optimized value of briquette shrinkage parameters at different reaction temperatures.

T (°C)	Time (h)	E (J mol^{-1})		$A_0 \times 10^{-3}$		n	
		Theoretical value	Optimized value	Theoretical value	Optimized value	Theoretical value	Optimized value
450	0–2	56,077	56,077	0.910	0.956	2.580	2.709
	2–5	2618	2618	5.694	5.352	0.625	0.625
	5–5.8	6271	6271	21.388	21.388	0.165	0.165
550	0–1.25	11,585	11,237	0.132	0.140	2.819	2.650
	1.25–3	622	622	3.687	3.834	0.946	0.946
	3–4.5	4524	4524	13.636	13.636	0.129	0.129
650	0–0.5	10,643	10,643	0.936	0.936	2.838	3.008
	0.5–2	216	216	5.868	5.457	1.306	1.397
	2–3	5005	5005	7.695	6.849	0.694	0.756
850	0–0.5	9140	10,237	0.081	0.072	2.970	3.297
	0.5–0.85	2546	2546	1.748	1.748	1.010	1.010
	0.85–1.4	5800	5800	3.518	3.518	0.457	0.457

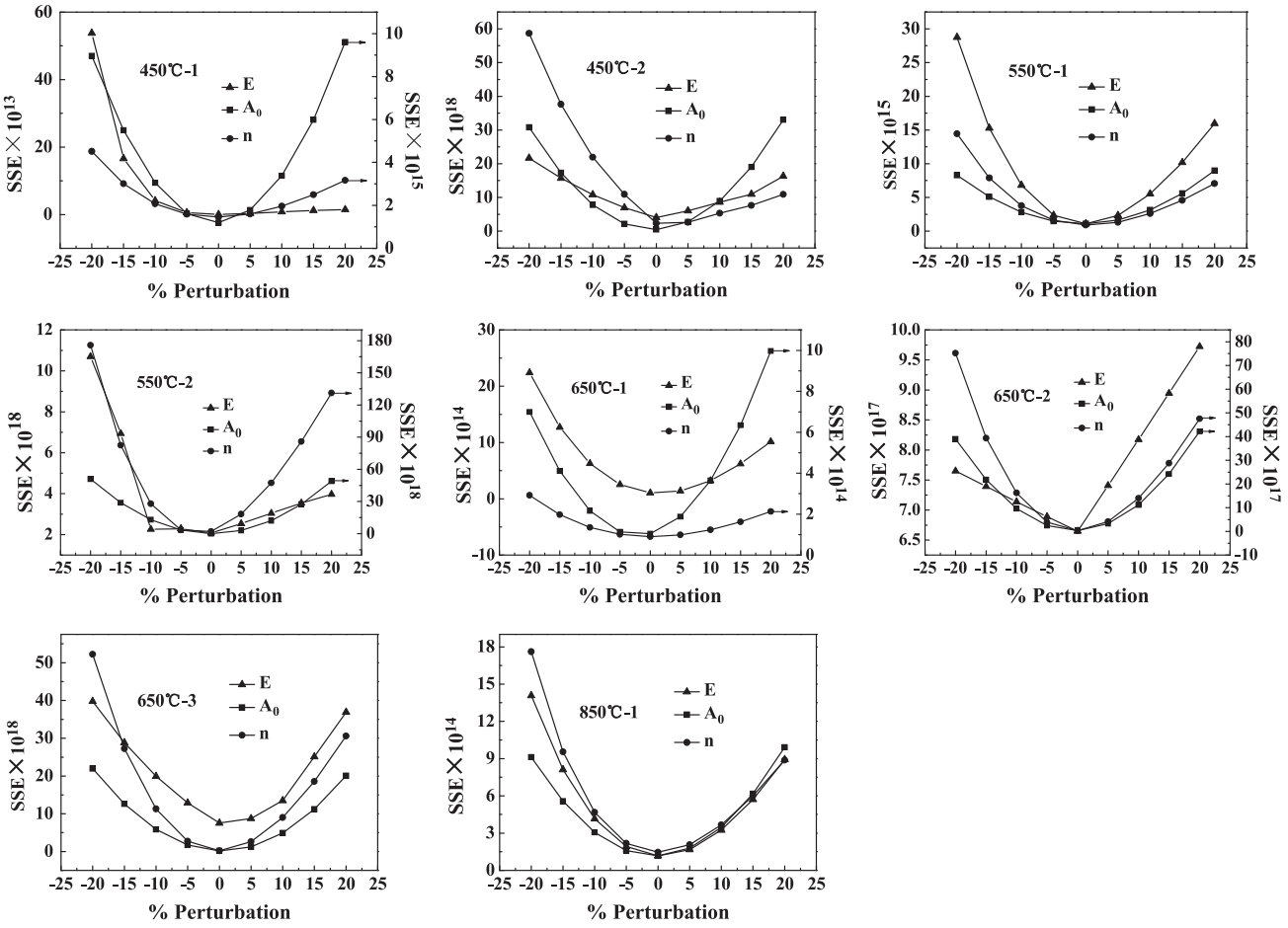

Fig. 7. Sensitivity analysis of optimized kinetic parameters at different temperatures and during different time period.

under the same temperature with side-length (100 mm). The briquette shrinkage rate of coal in the carbonization chamber was obtained by weighting the shrinkage parameters of volume units under different temperatures.

The briquette shrinkage rate could be obtained from Eq. (4), where the volume shrinkage rate of coal labeled i and $a - i + 1$ at time t is shown in Eq. (14):

$$dV'_{ti}/dt = V'_{0i}[(1 - x_i)d\beta_i/dt - k_i(1 - x_i)^n\beta_i] \quad (14)$$

where the volume changing parameter is

$$\beta_i = V'_{ti}/[V'_{0i}(1 - x_i)] \quad (15)$$

the volume shrinkage rate of coal in the combustion chamber is

$$dV'_t/dt = \frac{1}{5} \times \sum_{1}^{5} dV'_{ti}/dt \quad (16)$$

and the volume change coefficient of coal in the combustion chamber is

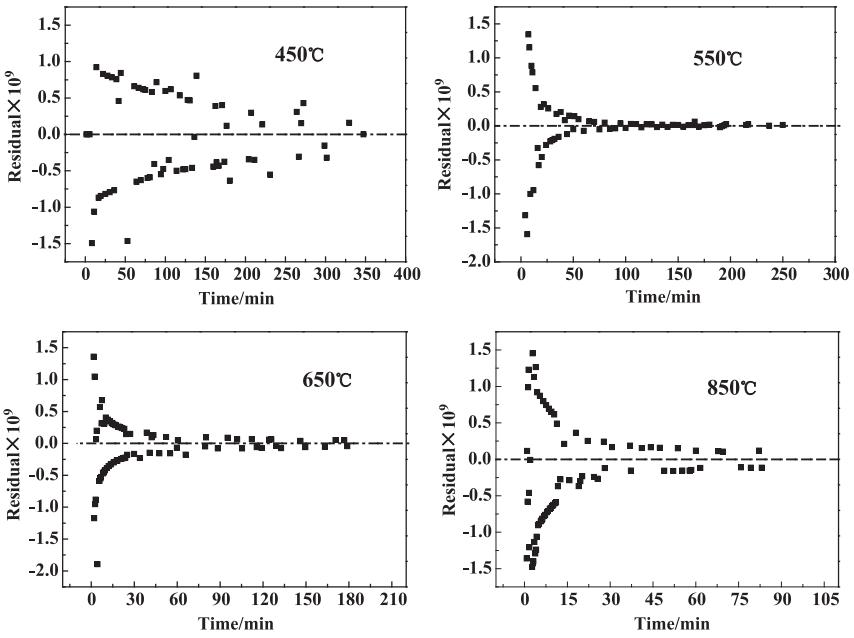

Fig. 8. Residual analysis of kinetic parameters at different temperatures.

$$\beta_t = V'_t / \left[V'_0 \left(1 - \frac{1}{5} \times \sum_{1}^{5} x_{ti} \right) \right] \tag{17}$$

3.2.2. Verification of the carbonization chamber shrinkage model

According to the volume change regulations of large-size briquette at different carbonization temperatures and time periods, the volume of coal labeled i and $a - i + 1$ at different temperatures at different carbonization temperatures and time periods were obtained and the estimated value of volume shrinkage rate for tamped coke in champers were acquired then. According to the conversion x, the Arrhenius coefficient k, the reaction order n, volume changing parameter β, and the differential of volume changing parameter $\frac{d\beta}{dt}$ of large-size briquette at different carbonization temperatures and stages, the conversion x_i, the Arrhenius coefficient k_i, the reaction order n_i, volume changing parameter β_i, and the differential of volume changing parameter $\frac{d\beta_i}{dt}$ of tamped coke labeled i and $a - i + 1$ at different temperatures were calculated, and the theoretical value of volume shrinkage rate for tamped coke in champers were acquired further. The coal and coke positions were measured in the tamped coke oven and the volume change regulations of tamped coke in champers was calculated, and the

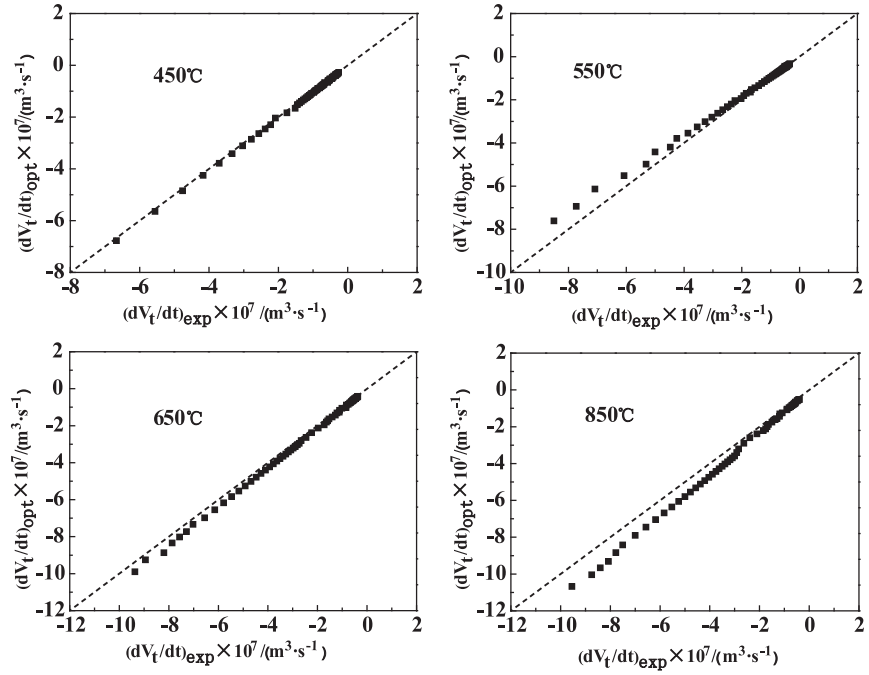

Fig. 9. Parity plots of kinetic parameters at different temperatures.

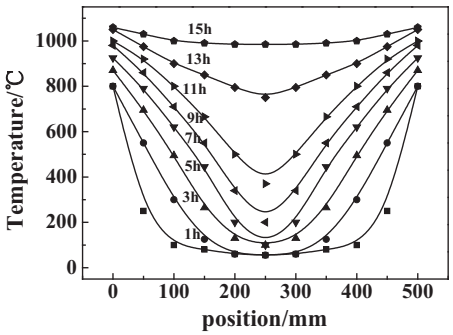

Fig. 10. Temperature distribution of coal in carbonization chamber.

Table 8
The average temperature of tamped coke labeled i and $a - i + 1$ during different time period.

Time (h)	T_{1+10} (°C)	T_{2+9} (°C)	T_{3+8} (°C)	T_{4+7} (°C)	T_{5+6} (°C)
1	550	525	175	75	50
3	800	650	450	200	75
5	825	775	600	375	200
7	885	825	700	500	300
9	950	915	775	625	450
11	990	960	860	750	600
13	1010	1000	940	900	820
15	1035	1035	1010	990	980

Table 9
V_t/V_0 of briquette at different temperatures and during different carbonation time periods.

Temperature (°C)	V_t/V_0				
	0–1 h	1–3 h	3–13 h	13–15 h	>15 h
⩽350	1	1	1	–	–
400	1	0.881	0.881	–	–
450	$0.0107t^2 - 0.0819t + 1.0022$	0.881	0.875	–	–
500	$0.0160t^2 - 0.1045t + 1.0024$	0.857	0.848	–	–
550	$0.0213t^2 - 0.1271t + 1.0027$	0.833	0.825	–	–
600	$0.0457t^2 - 0.1844t + 0.9909$	0.805	0.805	–	–
650	$0.0702t^2 - 0.2417t + 0.9791$	0.777	0.769	–	–
700	$0.0882t^2 - 0.2727t + 0.9827$	0.776	0.768	–	–
750	$0.1061t^2 - 0.3036t + 0.9864$	0.774	0.768	0.768	–
800	$0.1241t^2 - 0.3346t + 0.9900$	0.773	0.767	0.767	0.767
850	$0.1686t^2 - 0.3901t + 0.9965$	0.767	0.767	0.767	0.767
⩾900	$0.2431t^2 - 0.4516t + 0.9753$	0.767	0.767	0.767	0.767

experimental value of volume shrinkage rate for tamped coke in champers are acquired further. The calculation procedures of established, theoretical and experimental value were explained in Sections 3.2.2.1 (calculation of estimated value), 3.2.2.2 (calculation of theoretical value) and 3.2.2.3 (calculation of experimental value) below respectively.

3.2.2.1. The calculation of estimated value. Fig. 10 shows the temperature distribution of coal in the carbonization chamber after different carbonization periods [31]. The average carbonization temperature of coal labeled i and $a - i + 1$ at different temperatures is shown in Table 8.

Table 9 shows ratios of V_t/V_0 for large-size briquette at different temperatures and time periods [32]. The relational expression between the shrinkage volume and time was fitted by the date within 1 h at different temperatures. When the temperature was in the 450–850 °C range, the briquettes shrank completely within 100–140 min. Thus, the volume was limited by the carbonization time in the range of 0–3 h, while the volume was the ultimate constraint under corresponding carbonization temperature in the range of 3–5 h. Because the reaction at 850 °C has less effect on the briquette shrinkage, the briquette volume at temperatures higher than 900 °C was similar to volumes at 850 °C.

Table 10
The V'_t/V'_0 of tamped coke labeled i and $a - i + 1$ and the estimated value of dV'/dt after different time period.

Time (h)	V'_{1+10}/V'_0	V'_{2+9}/V'_0	V'_{3+8}/V'_0	V'_{4+7}/V'_0	V'_{5+6}/V'_0	V'_{total}/V'_0	$\frac{dV'_t}{dt}_{est} \times 10^{-3}$ ($m^3\ min^{-1}$)
0	1	1	1	1	1	1	−4.75939
1	0.897	0.906	1	1	1	0.961	−2.37933
3	0.820	0.881	1	1	1	0.940	−3.09313
5	0.767	0.769	0.881	1	1	0.883	−2.69658
7	0.767	0.768	0.825	1	1	0.872	−2.30002
9	0.767	0.767	0.769	0.825	1	0.825	−2.97417
11	0.767	0.767	0.768	0.806	0.881	0.797	−2.30002
13	0.767	0.767	0.767	0.768	0.769	0.767	−1.18967
15	0.767	0.767	0.767	0.767	0.767	0.767	0

The following are examples of volume calculation procedures for coal in the carbonization chamber.

When the carbonization time was 1 h, the volume of tamped coke labeled i and $a - i + 1$ are calculated directly by bring the carbonization time into relational expressions.

When the carbonization time was 3 h, the temperature of the carbonization chamber close to the oven wall was at 800 °C; the temperature volume units labeled 1 and 2 at 800 °C were $V'_{1+10} = 0.773 \times (0.2V'_0)$, and the average temperature volume units labeled 2 and 9 at 450 °C were $V'_{2+9} = 0.881 \times (0.2V'_0)$.

The volume units labeled 3 and 8 were $V'_{3+8} = 1 \times (0.2V'_0)$,
the volume units labeled 4 and 7 were $V'_{4+7} = 1 \times (0.2V'_0)$,
and the volume units labeled 5 and 6 were $V'_{5+6} = 1 \times (0.2V'_0)$.
Three hours later, the volume of the briquette in the carbonization chamber was
$V'_{total} = (0.773 + 0.881 + 1 + 1 + 1)/5 = 0.931V'_0 \ldots$.

The V'_t/V'_0 of coal labeled i and $a - i + 1$ after different time periods were calculated in the same way, and the estimated value of volume shrinkage rate $\frac{dV'_t}{dt}_{est}$ was obtained then, the results are shown in Table 10.

3.2.2.2. The calculation of theoretical value. According to the briquette volume conversion at different temperatures [32], the conversion x_i of coal during different time periods and at different temperatures is shown in Table 11.

The examples of the calculation procedures for the conversion of coal in the carbonization chamber can be seen below.

Fig. 10 shows the initial temperature of the oven wall liner was 1100 °C, and the coal was placed into the carbonization chamber at room temperature. Thus, the volume unit labeled 1 and 10 was at 550 °C (1100 ÷ 2), and the conversion value at 550 °C was:

$x_{1+10} = 0.2295 \times \ln 3600 - 1.1135 = 0.766$
the volume unit labeled 2 and 9 at 500 °C had a conversion value of
$x_{2+9} = 0.1954 \times \ln 3600 - 0.9237 = 0.676$,
the volume unit labeled 3 and 8 at 250 °C had a conversion of $x_{3+8} = 0.36$,
the volume unit labeled 4 and 7 at 150 °C had a conversion value of $x_{4+7} = 0.15$,
and the volume unit labeled 5 and 6 at 50 °C had a conversion of $x_{5+6} = 0$.

Table 11
x_i at different temperatures and during different time period.

Temperature (°C)	x_i			Fitting time (h)
	0–1 h	1–3 h	>5 h	
50	0	0.1033lnt − 0.5311	0.1310lnt − 0.7303	1.5
100	0.07	0.1117lnt − 0.5685	0.1347lnt − 0.7534	1.7
150	0.15	0.1201lnt − 0.6058	0.1438lnt − 0.7765	2.0
200	0.26	0.1285lnt − 0.6431	0.1502lnt − 0.7996	2.5
250	0.36	0.1369lnt − 0.6805	0.1566lnt − 0.8227	3.0
300	−0.0433lnt + 0.4045	0.1453lnt − 0.7178	0.1630lnt − 0.8458	4.0
350	0.0249lnt + 0.0250	0.1536lnt − 0.7551	0.1694lnt − 0.8689	6.5
400	0.0931lnt − 0.3545	0.1704lnt − 0.8300	0.1822lnt − 0.9151	6.2
450	0.1613lnt − 0.7340	0.1871lnt − 0.9044	0.1950lnt − 0.9613	6.0
500	0.1954lnt − 0.9237	0.2039lnt − 0.9791	0.2078lnt − 1.0075	4.5
550	0.2295lnt − 1.1135	0.2206lnt − 1.0537		3.0
600	0.1873lnt − 0.8600	0.1916lnt − 0.8801	0.1994lnt − 0.9361	3.8
650	0.1452lnt − 0.6066	0.1626lnt − 0.7065	0.1781lnt − 0.8185	4.5
700	0.1566lnt − 0.7225	0.1705lnt − 0.7065	0.1821lnt − 0.7905	4.0
750	0.1679lnt − 0.7110	0.1783lnt − 0.7065	0.1861lnt − 0.7625	3.5
800	0.1793lnt − 0.6995	0.1861lnt − 0.7065	0.1900lnt − 0.7345	2.4
850		0.1940lnt − 0.7065		1.8
⩾900		0.1999lnt − 0.6925		1.5

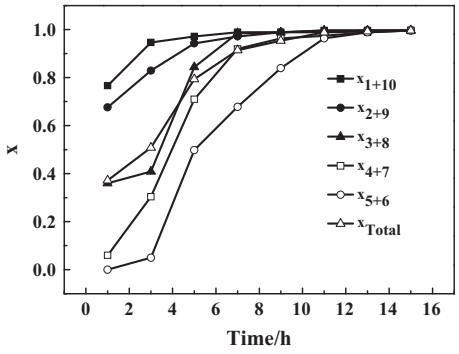

Fig. 11. The conversion x_i of tamped coke labeled i and $a - i + 1$ after different time period.

When the carbonization time was 3 h, the calculation procedures for the conversion of coal were the following.

Fig. 10 shows the temperature of the oven wall was approximately 800 °C after 3 h. Thus, the volume unit labeled 1 + 10 was at 800 °C. This part is under 550 °C before 1 h, and whose conversion value is 0.7658, which equaled the reaction time t = 0.9838 h (0.1793lnt − 0.6995 = 0.7658) at 800 °C; at this point, the coal had completed the reaction, and the conversion at this stage was zero. The conversion of coal labeled i and $a - i + 1$ during different time period was calculated in the same way, and list in Fig. 11.

As the same calculation method for the conversion of the tamped coke labeled i and $a - i + 1$, the reaction order n_i, the Arrhenius coefficient k_i, volume changing parameter β_i, and the differential of volume changing parameter $\frac{d\beta_i}{dt}$ of tamped coke labeled i and $a - i + 1$ at different temperatures were calculated according to the

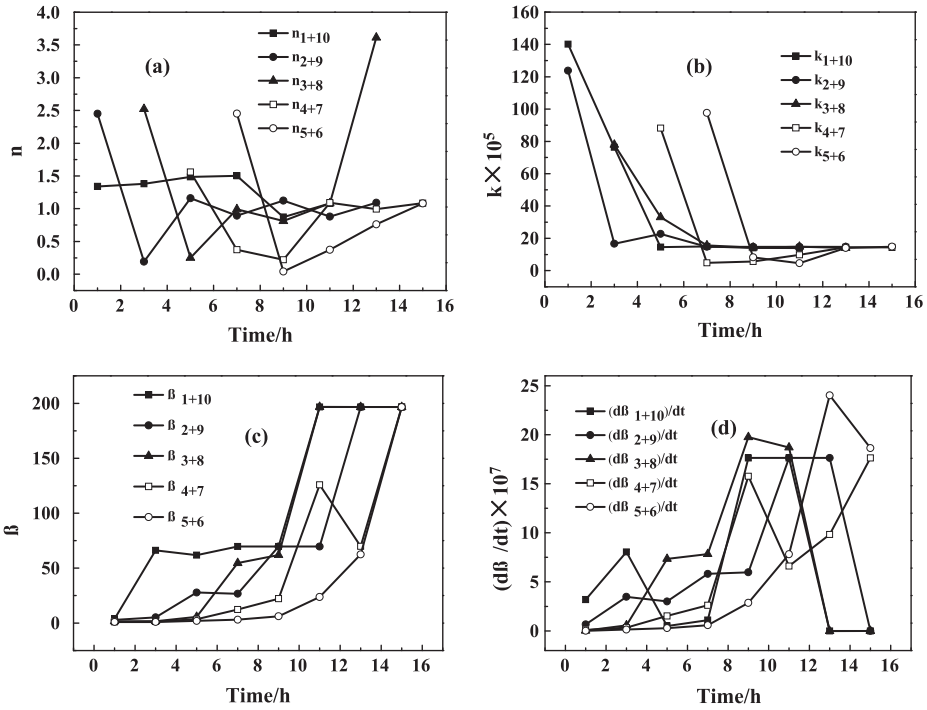

Fig. 12. The reaction order n_i (a), Arrhenius coefficient k_i (b), volume changing parameter β_i (c), and the differential of volume changing parameter $\frac{d\beta_i}{dt}$ (d) of tamped coke labeled i and $a - i + 1$ after different time period.

Table 12
The dV'_i/dt of tamped coke labeled i and $a - i + 1$ and the theoretical value of dV'_i/dt after different time period.

Time (h)	$\frac{dV_{i-1|0-i+1}}{dt} \times 10^{-6}$ ($m^3 \cdot min^{-1}$)					$\frac{dV'}{dt_{the}} \times 10^{-3}$ ($m^3 \cdot min^{-1}$)
	$i = 1$	$i = 2$	$i = 3$	$i = 4$	$i = 5$	
1	-1221.397	−396.587	0	0	0	−1.618
3	−1031.013	−1085.889	−947.527	0	0	−3.064
5	−420.343	−896.133	−1392.138	0.017	0	−2.708
7	0.011	−11.706	−888.253	−1393.28	0.046	−2.293
9	0.228	−3.997	−451.807	−1542.094	−948.212	−2.946
11	0.171	0.228	−12.049	−452.092	−1835.151	−2.299
13	0	−0.114	−3.997	−305.449	−900.644	−1.210
15	0	0	0	0.057	−23.812	−0.024

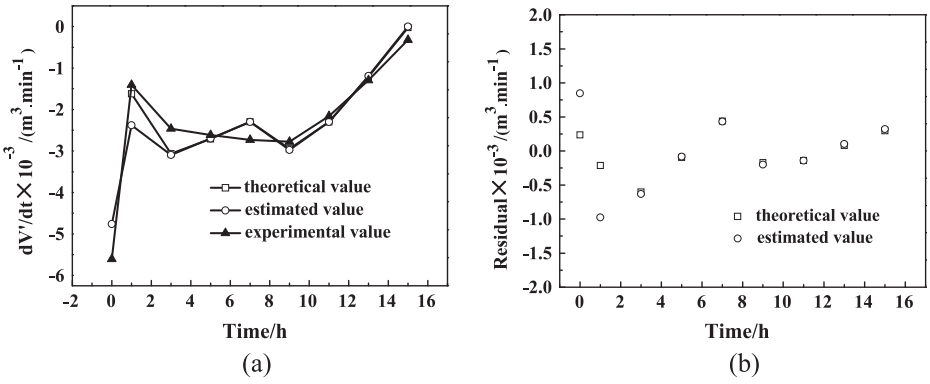

Fig. 13. Comparison of the theoretical, estimated and industrial value for the shrinkage rate of tamped coke in carbonization chamber: (a) shrinkage rate curves and (b) residual analysis.

kinetic parameters of large-size briquette at the same carbonization [32] and the carbonization temperatures and stages of the tamped coke. The results are shown in Fig. 12.

Put the kinetic parameters of tamped coke labeled i and $a - i + 1$ into Eq. (14), the theoretical value of volume shrinkage rate for tamped coke after different carbonization time was obtained.

When the temperature was lower than 100 °C, the coal had not undergone the moisture evaporation reaction, the volume of coal did not change, and the volume shrinkage rate was set to zero; when the temperature was higher than 900 °C, the volume of the coal change little, and the volume shrinkage rate was set to zero (see Table 12).

3.2.2.3. The calculation of experimental value. The coal and coke positions were measured in the tamped coke oven and the volume change regulations of tamped coke in champers was calculated, and the experimental value of volume shrinkage rate for tamped coke in champers were acquired further (Fig. 13a). Residual analysis is employed to compare the difference among the estimated value, theoretical value and experimental value.

The variation regulation of the theoretical, estimated and experimental value for the carbonization chamber coal shrinkage rate is shown in Fig. 13. All three values were in agreement. The shrink regulations of tamped coal cakes in carbonization chambers are consistent with the large-sized briquettes.

However, the shrinkage rate curve of the tamped coal cakes in the carbonization chamber was smaller than for the large-sized briquettes because of the large temperature gradient of different coal types in the carbonization chamber. Specifically, the instantaneous shrinkage rate of the coal material at high temperatures in the carbonization furnace rose by 6×10^{-3} m^3/min from zero at the initial time point. When the reaction was stable, the shrinkage rate decreased rapidly. The dehydration and degassing, thermal decomposition, and the condensation reactions occurred during the pyrolysis process, and the shrinkage rate increased gradually; the gas precipitation amount decreased in the later reaction stage, and the shrinkage rate gradually returned to zero. However, the shrinkage rate curve of the tamped coal cake in the carbonization chamber was smaller than for the large-sized briquettes because of the large temperature gradient between the different coal types in the carbonization chamber.

4. Conclusion

(1) In the process of the carbonization, the dehydration and degassing reactions before reaching 450 °C and the polycondensation reaction in the range of 550–650 °C were the primary causes of briquette shrinkage during the carbonization process; the leakage of gas decreased after 850 °C, which had the least effect on the briquette volume shrinkage. There were three main reasons causing the shrinkage of large-size briquette: the decrease of coal volume caused by the volatilization of moisture and volatiles, the decrease of coal volume caused by the pyrolysis reaction and the density increase of briquette caused by the decrease of coal volume.

(2) The briquette shrinkage kinetic model was represented as follows: $dV_t/dt = V_0[(1-x)d\beta/dt - A_0 e^{-E/RT}(1-x)^n\beta]$; There was a positive correlation between the volume changing parameter β and the density of briquette, and the volume changing parameter increased with the reaction; the shrinkage reaction was divided into three stages; with the reaction went on, the reaction order and reaction rate constant decreased, the pre-exponential factor increased and the activation energy decreased firstly and increased then. The pyrolysis kinetic parameters of briquette was calculated on the basis of mass loss change regulation, while the shrinkage

kinetic parameters of briquette was calculated on the basis of the volume change regulation; different kinetic model basis was the main reason that cause the difference between the kinetic parameter change regulation of the two kinetic model.

(3) The shrinkage of the tamped coal cakes from the large-scale chamber was counted in the calculated unit whose thickness was 100 mm. The shrinkage velocity of the tamped coal cakes in carbonization chamber was obtained by weighted calculating the shrinkage parameters of each volume unit at different temperatures, and the volume shrinkage calculation method of the tamped coal cake (13,280 mm × 500 mm × 4300 mm) was obtained. The shrink regulations of the tamped coal cake in the carbonization chamber were consistent with the large-sized briquettes. However, the shrinkage rate curve of the tamped coal cake in the carbonization chamber was smaller than the large-sized briquette because of the large temperature gradient of the different coal types in the carbonization chamber.

Acknowledgments

This work was supported by the National Natural Science Foundation of China (Grant No. 51274147), the National Science & Technology Pillar Program (Grant No. 2012BAA04B03), the Shanxi Provincial Natural Science Foundation (2010011014-1) and 2014 Shanxi Provincial Postgraduate innovation program.

References

[1] Ha S, Li Y, Zhang H, Shi HY, Zhu C. Study on a separation technology for more efficient utilization of pulverized coals in cement plants. Fuel Process Technol 2010;91:1261–6.
[2] Liu JX, Jiang XM, Han XX, Shen J, Zhang H. Chemical properties of superfine pulverized coals. Part 2. Demineralization effects on free radical characteristics. Fuel 2014;115:685–96.
[3] Alonso M, Borrego A, Alvarez D, Menéndez R. Pyrolysis behaviour of pulverised coals at different temperatures. Fuel 1999;78:1501–13.
[4] Bongers GD, Jackson WR, Woskoboenko F. Pressurised steam drying of Australian low-rank coals: Part 2. Shrinkage and physical properties of steam dried coals, preparation of dried coals with very high porosity. Fuel Process Technol 2000;64:13–23.
[5] Fu ZX, Guo ZC, Yuan ZF, Wang Z. Swelling and shrinkage behavior of raw and processed coals during pyrolysis. Fuel 2007;86:418–25.
[6] British Coke Research Association. The effect of rate of carbonization and of coal rank on the characteristics of the cokes produced. In: Coke research, report 24; 1963.
[7] Echterhoff H, Beck K, Peters W. Size distribution, strength and reactivity of coke and how they are affected by the coking process. In: Blast furnace, coke oven & raw materials conference; 1961. p. 403–18.
[8] Nomura S, Arima T. Effect of coke contraction on mean coke size. Fuel 2013;105:176–83.
[9] Chang HZ, Zeng FG, Li WY. Semicoke contraction kinetics of coal and its macerals in pyrolysis. Acta Phys Chim Sin 2008;24:675–80.
[10] Chapter 5. Coal composition and reservoir characterization, coal and coal bed gas; 2014. p. 235–99.
[11] Gu JF. The characteristics of dilatation and contraction of the cold-pressed briquette during carbonization. Coal Chem Ind 1996;1:37–43.
[12] Fernández A, Barriocanal C, Alvarez R. The effect of additives on coking pressure and coke quality. Fuel 2012;95:642–7.
[13] Gransden JF, Khan MA, Price JT. Coking pressure and coke quality at different locations in an industrial oven. In: 47th Iron making conf proc; 1988. p. 155–62.
[14] Fu ZX, Guo ZC, Yuan ZC. Shrinkage characteristics of briquette during pyrolysis using online images collection. J Fuel Chem Technol 2005;33(5):525–9.
[15] Alvarez R, Diez M, Barriocanal C, Díaz-Faes E, Cimadevilla J. An approach to blast furnace coke quality prediction. Fuel 2007;86:2159–66.
[16] Sato H, Aoki H, Miura T, Patrick JW. Estimation of thermal stress in lump coke. Fuel 1997;76:303–10.
[17] Bei KL, Wang P, Zhang YF. Study on blended coal coking and shrinkage at temperature gradient. Coal Convers 2006;29(1):49–52.
[18] Chen Y, Wang X, He R. Modeling changes of fractal pore structures in coal pyrolysis. Fuel 2011;90:499–504.
[19] Snape CE. Similarities and differences of coal reactivity in liquefaction and pyrolysis. Fuel 1991;70:285–8.
[20] Jenkins D, Mahoney M, Keating J. Fissure formation in coke. 1: The mechanism of fissuring. Fuel 2010;89:1654–62.
[21] Zhao YQ, Zhang YF, Liang Y. Crack formation characteristic of "ball structure" carbonized briquette. In: 2013 International conference on coal science & technology, PA, United States; 2013.
[22] Jenkins D, Mahoney M. Fissure formation in coke. 2: Effect of heating rate, shrinkage and coke strength. Fuel 2010;89:1663–74.
[23] Jenkins D, Shaw D, Mahoney M. Fissure formation in coke. 3: Coke size distribution and statistical analysis. Fuel 2010;89:1675–89.
[24] Wang Q, Zhang YF, Zhao YQ. Study on shrinkage characteristic of briquette during the pyrolysis process. In: 2013 International conference on coal science & technology, PA, United States; 2013.
[25] Alcázar LA, Ancheyta J. Sensitivity analysis based methodology to estimate the best set of parameters for heterogeneous kinetic models. Chem Eng J 2007;128:85–93.
[26] Zhang YF, Zhang HR, Sun YL. The characteristics of anthracite briquette carbonization and the regularity of pyrolysis gas generation during carbonization. J China Coal Soc 2011;36(4):670–5.
[27] Wang ZL, Li GD. Experimental method and prediction model for autogenous shrinkage of high performance concrete. Constr Build Mater 2007;49:400–6.
[28] Sadhukhan AK, Gupta P, Saha RK. Modelling of combustion characteristics of high ash coal char particles at high pressure: shrinking reactive core model. Fuel 2010;89:162–9.
[29] Ulloa C, Gordon AL, García X. Distribution of activation energy model applied to the rapid pyrolysis of coal blends. J Anal Appl Pyrol 2004;71:465–83.
[30] Sonoyama N, Hayashi J. Characterisation of coal and biomass based on kinetic parameter distributions for pyrolysis. Fuel 2013;114:206–15.
[31] Zhang YF. The applied basic research and technology development of high rank coal or coke powder to make "ball structure" carbonized briquette. Shanxi Zhongyuan Coal Cleaning Technology Co.; 2012.
[32] Zhang HR. Characteristics of fine anthracite molding and briquette pyrolysis. China: Taiyuan University of Technology; 2011.